Microbial Pathogenesis 131 (2019) 218–226

Contents lists available at ScienceDirect

Microbial Pathogenesis

journal homepage: www.elsevier.com/locate/micpath

Characterization of serine acetyltransferase (CysE) from methicillin-resistant *Staphylococcus aureus* and inhibitory effect of two natural products on CysE

Changming Chen[a,1], Qiulong Yan[a,1], Mengxing Tao[a], Huaying Shi[a], Xiuyan Han[a], Liqiu Jia[a], Yukun Huang[a], Lizhe Zhao[a], Chao Wang[b], Xiaochi Ma[b], Yufang Ma[a,*]

[a] Department of Biochemistry and Molecular Biology, Dalian Medical University, Dalian, 116044, China
[b] College of Pharmacy, Dalian Medical University, Dalian, 116044, China

ARTICLE INFO

Keywords:
MRSA
Serine acetyltransferase
CysE
Natural products
Inhibitors

ABSTRACT

Methicillin-resistant *Staphylococcus aureus* (MRSA) is a major hospital-acquired infective pathogen that has developed resistance to many antibiotics. It is imperious to develop novel anti-MRSA drugs to control the emergence of drug resistance. The biosynthesis of cysteine in bacteria is catalyzed by CysE and CysK. CysE was predicted to be important for bacterial viability, it could be a potential drug target. The serine acetyltransferase activity of CysE was detected and its catalytic properties were also determined. CysE homology model was built to investigate interaction sites between CysE and substrate L-Ser or inhibitors by molecular docking. Docking data showed that residues Asp94 and His95 were essential for serine acetyltransferase activity of CysE, which were confirmed by site-directed mutagenesis. Colorimetric assay was used to screen natural products and six compounds which inhibited CysE activity (IC_{50} ranging from 29.83 μM to 203.13 μM) were found. Inhibition types of two compounds 4 (11-oxo-ebracteolatanolide B) and 30 ((4*R*,4a*R*)-dihydroxy-3-hydroxymethyl-7,7,10a-trimethyl-2,4,4a,5,6,6a,7,8,9,10,10a,l0b-dodecahydrophenanthro[3,2-*b*]furan-2-one) on CysE were determined. Compounds 4 and 30 showed inhibitory effect on MRSA growth (MIC at 12.5 μg/ml and 25 μg/ml) and mature biofilm. The established colorimetric assay will facilitate further high-throughput screening of CysE inhibitors from different compound libraries. The compounds 4 and 30 may offer structural basis for developing new anti-MRSA drugs.

1. Introduction

Staphylococcus aureus is an opportunistic pathogen, which can cause skin and soft-tissue infections, sepsis, and necrotizing pneumonia in the world [1,2]. Methicillin-resistant *Staphylococcus aureus* (MRSA) emerged in the 1960s, spreading rapidly due to the emergence of drug resistance to β-lactam antibiotics [3–5]. Moreover, MRSA clinical strains showed decreased susceptibility to vancomycin and became more resistant to daptomycin and linezolid [6,7]. As a consequence, it is a matter of urgency to find more effective candidates of novel anti-MRSA drugs.

Sulfur element is essential for life and plays a core role in numerous microbial metabolic processes. It is used in the biosynthesis of cysteine and methionine in its reduced form. Cysteine can be converted to important coenzymes and mycothiol involved in the redox defense [8–11]. The serine acetyltransferase (CysE) and O-acetylserine sulfhydrylase (CysK) involved in the biosynthetic pathway of cysteine had been characterized in *Escherichia coli*, *Salmonella typhimurium*, *Mycobacterium tuberculosis*, *Corynebacterium glutamicum* and *Entamoeba histolytica* [12–18]. However, the CysE and CysK of *Staphylococcus aureus* have not been identified. The amino acid sequences of CysE from seven bacterial species, *Staphylococcus aureus*, MRSA, *Escherichia coli*, *Salmonella typhimurium*, *Mycobacterium tuberculosis*, *Corynebacterium glutamicum* and *Entamoeba histolytica* were compared in this study (Fig. 1). The alignment results showed that the amino acids sequences of CysE highly conserved between MRSA and *Staphylococcus aureus*, but the low homology of CysE existed between MRSA and other bacterial species. Moreover, since microbial and plants sulfur metabolic pathways are largely absent in humans and CysE involved in the cysteine synthesis is essential [19], it is assumed that CysE could serve as a potential drug target for anti-*Staphylococcus aureus*. It is necessary to understand the catalytic mechanism of MRSA CysE and find inhibitors on MRSA CysE. *S. aureus* and MRSA are etiological intermediary to lead to countless human acute infections and their biofilm is the cause of chronic and

* Corresponding author. Department of Biochemistry and Molecular Biology, Dalian Medical University, 9 W. Lvshun South Road, Dalian, 116044, China.
E-mail address: yufang_ma@hotmail.com (Y. Ma).
[1] Both authors contribute equally to this work.

https://doi.org/10.1016/j.micpath.2019.04.002
Received 15 January 2019; Received in revised form 19 March 2019; Accepted 1 April 2019
Available online 09 April 2019

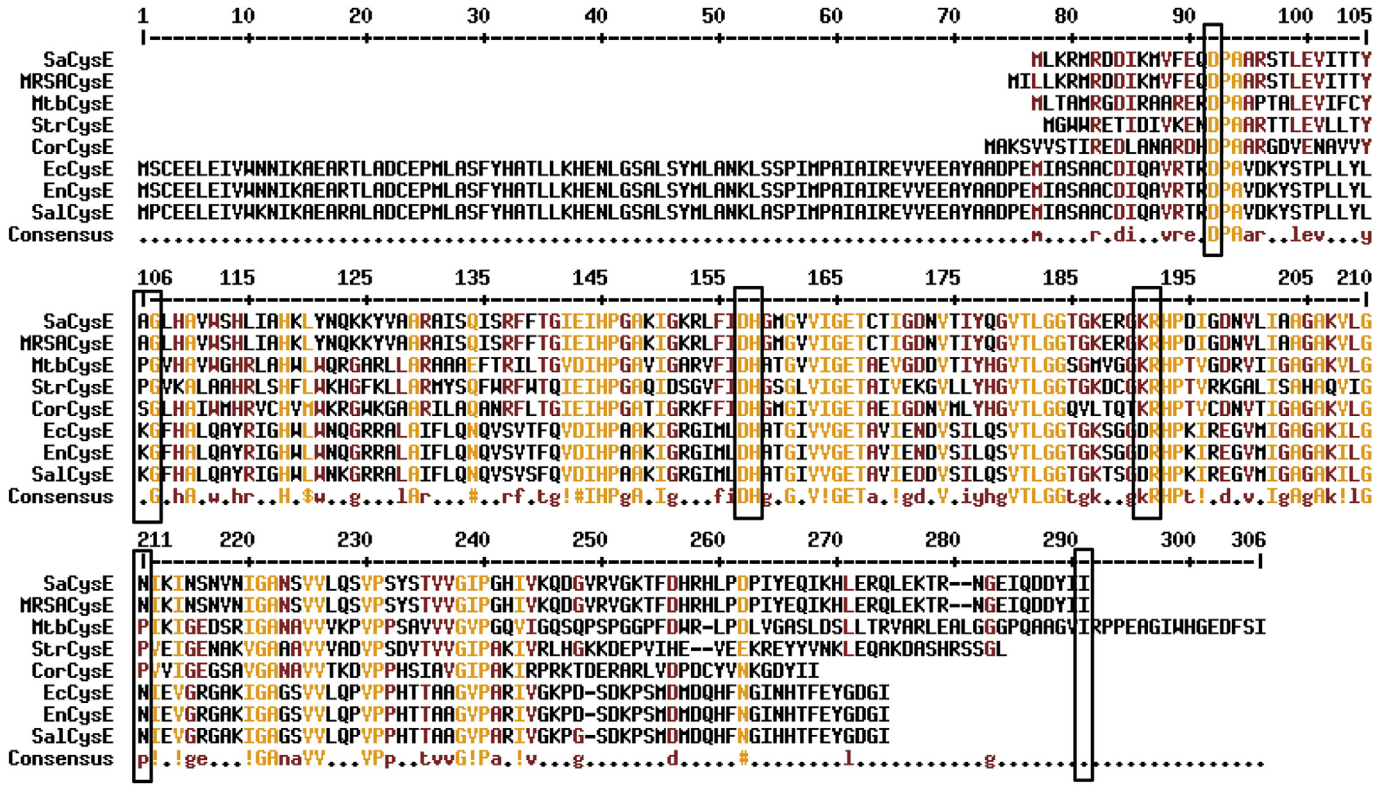

Fig. 1. Sequence alignment of CysE amino acids from seven bacterial species, *Staphylococcus aureus*, MRSA, *Escherichia coli*, *Salmonella typhimurium*, *Mycobacterium tuberculosis*, *Corynebacterium glutamicum* and *Entamoeba histolytica*. The highly conserved residues were showed in orange color and lowly conserved residues were presented in brown color. The residues of CysE which were predicted as the active sites with substrate L-Ser or compound 4 and 30 were signified in box. The symbols used in "Consensus" were as follows: "." means no consensus; an upper case abbreviation of an amino acids means a perfect consensus; a lower case abbreviation of an amino acids means an imperfect consensus where the amino acid was not present in all. (For interpretation of the references to color in this figure legend, the reader is referred to the Web version of this article.)

even recalcitrant disease [20,21]. Therefore, it is also needed to find inhibitors which are capable to effectively inhibit biofilm formation and/or destroy the biofilm.

In this study, MRSA *cysE* gene was cloned and MRSA CysE protein was expressed in *E. coli,* and purified CysE protein was obtained through Ni^{2+} affinity chromatography. The enzymatic activity of CysE protein was detected and the catalytic properties of CysE were determined. The colorimetric assay of CysE was developed to screen natural products and six CysE inhibitors were found as well as their action mechanism was explored in this study.

2. Materials and methods

2.1. Bacteria strains and plasmids

Methicillin-resistant *Staphylococcus aureus* (ATCC 33591) was obtained from American type culture collection, and it was used for preparation of genomic DNA. *Escherichia coli* NovaBlue (Novagen) was used for *cysE* gene cloning and BL21(DE3) (Novagen) for CysE protein expression, respectively. Cloning plasmid pJET1.2 blunt (Thermo) with ampicillin resistance gene was used for cloning of *cysE* gene. Expression vector pET29b (Novagen) carrying kanamycin resistance gene was utilized to express CysE protein in *E. coli* BL21(DE3).

2.2. Detection of serine acetyltransferase activity of CysE protein

MRSA genomic DNA was prepared as previously described [22]. MRSA *cysE* gene was amplified from MRSA genomic DNA by using forward primer, 5′ CCCCATATGATCTTGTTAAAAAGAATG 3' (underlined sequence is NdeI site) and reverse primer, 5′ CCCTCGAGTATAA TGTAATCATCTTGAATC 3' (underlined sequence is XhoI site). The amplified PCR product was ligated into pJET1.2 blunt vector to yield plasmid pJET-*cysE*. After confirmation by DNA sequencing, the *cysE* gene was ligated into the NdeI and XhoI sites of pET-29b (Novagen), resulting in pET29b-*cysE*. pET29b-*cysE* was transformed to *Escherichia coli* BL21(DE3) competent cells, generating a CysE expressing strain BL21(DE3)/pET29b-*cysE*.

BL21(DE3)/pET29b-*cysE* was cultured in LB broth with 50 μg/ml kanamycin and induced with 1 mM isopropyl-D-thiogalactopyranoside (IPTG) at 30 °C for 6 h. The cells were harvested and suspended in lysis buffer (20 mM Tris-HCl, pH 8.0, 500 mM NaCl, 25 mM $MgCl_2$, 20% glycerol, 1 mM EDTA and 1 mM PMSF) followed by sonication. After centrifugation at 20,000 × *g* for 15 min, the supernatant was applied to Ni-NTA superflow column (Qiagen) and the column was then washed with 20 ml wash buffer (lysis buffer with 25 mM imidazole). CysE protein with a His-tag at its C-terminus was eluted by 10 ml elution buffer (lysis buffer with 200 mM imidazole) and the first 5 ml elution fraction was collected for further experiments. The concentration of CysE protein was determined by Bradford method, using bovine serum albumin (BSA) as standard. The purified CysE protein was detected by 15% SDS-PAGE and Western blotting.

The serine acetyltransferase activity of CysE protein was detected by both DTNB [5, 5′-dithiobis-(2-nitrobenzoic acid)] colorimetric assay and HPLC assay [13,23]. For colorimetric assay, the reaction condition was the same as above. The reaction was stopped with stop solution containing 50 mM Tris-HCl (pH 7.5) and 6 M guanidine hydrochloride. After adding colorimetric reagent solution containing 0.2 mM DTNB, the SH- group of CoA turned DTNB to NTB^- which absorbance at wavelength of 405 nm was read using a microplate reader. The control containing all components except CysE protein was used to correct the

errors from the -SH group of CysE and positive control containing 0.2 mM CoA was used for calculating the amount of CoA produced in reactions. All experiments were performed in triplicate.

The Z′ factor had been proposed a value to estimate the quality of the assay itself in high-throughput screening [24–26]. To evaluate the sensitivity and reproducibility of the assay, the statistical parameter Z' value was calculated. The reaction with CysE was positive control, and the reaction without CysE was negative control.

For HPLC assay, the reaction mixture containing 0.4 μg CysE, 5 mM $MgCl_2$, 50 mM Tris-HCl (pH 7.5), 2 mM L-serine (L-Ser) and 0.4 mM acetyl coenzyme A (AcCoA) was incubated at 37 °C for 20 min. The mixture was then injected into Nova-Pak C18 column (3.9 × 150 mm; Waters, Manchester, UK). The mobile phase was 20 mM KH_2PO_4 (pH6.5)-methanol (95:5) with 0.8 mL/min flow rate at 25 °C. The product CoA was monitored at 259 nm.

2.3. Kinetic properties of CysE

The kinetic properties of CysE were determined using above-mentioned colorimetric assay. The initial velocity of CysE was determined by performing the reactions at variable CysE concentrations and different incubation times. The reaction for enzyme concentration-curve was carried out in reaction buffer with different concentrations of CysE (2, 4, 6, 8 and 10 μg/ml) at 37 °C for 5, 10 and 15 min. Time-course curves were plotted by calculating the amount of CoA at different reaction times (3, 5, 10, 15 and 20 min) with varying concentrations of CysE (4, 6 and 8 μg/ml) at 37 °C. In the range of initial velocity, the optimal pH, temperature, and the effect of 4 cations on CysE were determined by setting variable pH buffers (4–10), different temperatures (16–80 °C) and different concentrations of Mg^{2+}, Ca^{2+}, Ba^{2+} and K^+ (0–20 mM), respectively. In dual-substrate reactions, the steady-state kinetic parameters K_m and V_{max} of AcCoA were determined by double reciprocal plots prepared by various concentration of AcCoA (0.04–0.2 mM) while L-Ser was in excess (2 mM) under optimal conditions, and the K_m and V_{max} of L-Ser were measured by different concentration of L-Ser (0.2–1.6 mM) with AcCoA at a saturated concentration (0.2 mM). All experiments were performed in triplicate.

2.4. Homology model building and molecular docking

In accordance with the default parameter values, the homology model of CysE was built using SWISS-MODEL (http://swissmodel.expasy.org/). 4hzd.1.A (PDB ID) was used as a template of the homology model. Structural Analysis and Verification Server (version 4) (http://services.mbi.ucla.edu/SAVES/) were used to assess the predicted model. The molecular docking program Autodock (version 4.2) was used for docking analysis of CysE and its substrate L-Ser [27]. The docking gridbox of receptor was also set by Autodock, whose number grid points in XYZ is 126 × 126 × 126, and spacing is 0.375 Å. The Lamarckian Genetic Algorithm (LGA) of Autodock was selected as simulated method. The docking results were visualized by PyMol, LIGPLOT and DSViewer Pro 5.0 programs [28].

2.5. Site-directed mutagenesis

In order to investigate the catalytic mechanism of CysE, six amino acid residues (Asp29, Asp94, His95, Lys128, Arg129 and Asn148) of CysE, which were predicted to be important for binding with L-Ser, were substituted to alanine using MutanBEST Kit (Takara). All CysE mutant proteins were expressed, purified, quantified and their enzymatic activity was determined.

2.6. Screening of CysE inhibitors

The DTNB colorimetric assay of CysE was developed for high-through screening of CysE inhibitors. The natural products with single component prepared from different chinese herbal medicine in our previous studies, e.g. *Euphorbia fischeriana* and *Euphorbia ebracteolata* were dissolved in DMSO solvent [29]. The CysE was pre-incubated with different compounds on ice for 5 min and then CysE activity was detected. The enzyme reaction only containing DMSO solvent was used as a negative control. All experiments were performed in triplicate.

2.7. Resazurin assay

To test whether the compounds had inhibitory effect on growth of MRSA, an resazurin assay was used as described [30,31]. The resazurin dye is able to indicate the bacterial growth and metabolism based on the color conversion of the dye from blue to pink. The 50 μl Tryptic Soy Broth (TSB) medium containing compounds at the final concentrations from 1.56 μg/ml to 200 μg/ml was added in the 96-well plates. The MRSA culture suspension (2×10^6 cfu/ml) was prepared by mixing bacterial stock with TSB medium and 50 μl of culture suspension was then added into above wells. The wells containing DMSO and the culture were used as controls. After the culture was incubated for 12 h in a 37 °C incubator, 100 μl of 0.01% resazurin solution was added to each well and the color of culture was observed after an additional 3–5 h of incubation. If the resazurin color remained blue, bacterial growth was considered to be inhibited. The lowest concentration of the compounds at which bacterial growth was inhibited was considered as minimum inhibitory concentrations (MIC). Vancomycin and clindamycin (Aladdin), the effective antibiotics for treating MRSA, were used as positive controls in this experiment.

2.8. Effects of compounds on the growth of MRSA

MRSA was grown in TSB medium at 37 °C and the cultures were treated with different inhibitors at 1 × MIC and 2 × MIC respectively when the OD_{595} of cultures reached 0.3. Then the OD_{595} of cultures was measured at the interval of 1 h, moreover, 10 μl of cultures were taken for determining colony forming unit (CFU) at every time point. CFU/ml = colony number × dilution multiple × 100. All experiments were performed in triplicate.

2.9. Inhibition types of CysE inhibitors

To investigate the inhibition types of inhibitors on CysE, CysE reactions with different compounds at IC_{50} and two folds of IC_{50} were performed respectively. The inhibitory constant (Ki) and inhibition types were determined by double reciprocal plots. Molecular docking was also used to analyze the interaction of CysE and its inhibitors.

2.10. Biofilm assay

In order to determine whether the two inhibitors had inhibitory effect on MRSA biofilm, biofilm assay was performed. MRSA was grown in TSB at 37 °C until the OD_{595} of the culture reached 0.6. The 100 μl culture was then added into each well of PVC plate and incubated at 37 °C. Once formed, biofilm was washed three times by 0.1 mM PBS to remove planktonic cells. The fresh TSB medium with different inhibitors was then added into the formed biofilm respectively. After incubation for 24 h, crystal violet staining was applied to detect the effect of those two inhibitors on mature biofilm. The wells only containing DMSO were used as controls.

2.11. Cytotoxicity assay

The 3-[4, 5-dimethylthiazol-2yl]-2, 5-dipheny tetrazolium bromide (MTT) assay and TransDetect™ Cell Counting Kit (CCK) assay were utilized to test the cytotoxicity of two inhibitors on RAW264.7 and THP-1 macrophage cells separately. RAW264.7 cells were grown in the wells of 96-well plate containing DMEM medium plus 10% fetal bovine

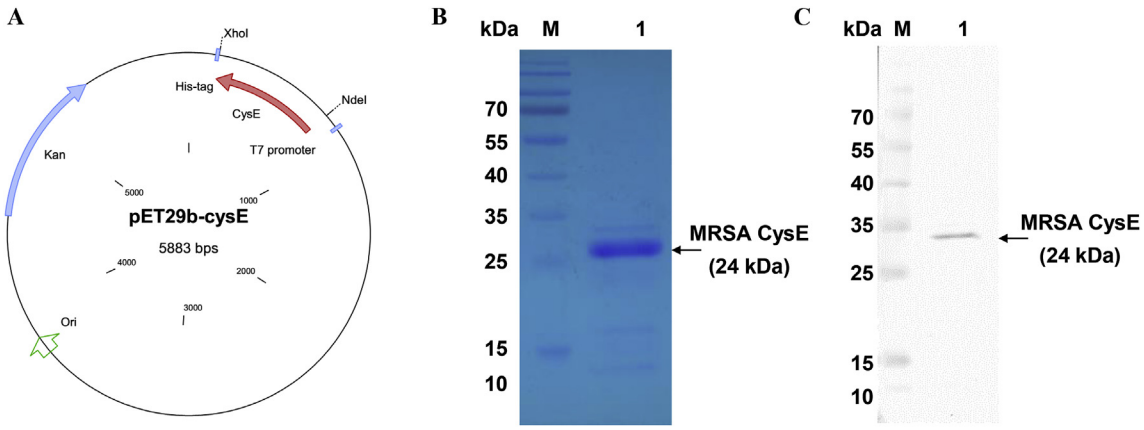

Fig. 2. Map of pET29b-*cysE* (A) and analysis of CysE protein by SDS-PAGE (B) and Western blot (C). M. PageRuler™ Prestained Protein Ladder; Lane 1. The purified CysE protein with an expected molecular weight of 24 kDa.

serum (FBS), while THP-1 cells were grown with RPMI 1640 medium plus 10% FBS. The medium containing different concentration of compounds was then added to the culture followed by incubation for 2 days. MTT was added in each well for additional 4 h incubation and OD_{595} was read by a microplate reader. While CCK was added in the wells, the OD_{450} was read. The medium containing DMSO was used as control.

2.12. Statistical analysis

Statistical analysis of experimental groups was performed using unpaired two-tailed *t*-test by GraphPad Prism v.6.01 software. All measurements were presented as the mean ± SD obtained from three independent experiments to correct the trial errors.

3. Results

3.1. Expression and purification of CysE protein

Expression vector pET29b-*cysE* was constructed and its map was shown in Fig. 2A. The soluble CysE protein with His-tag at its C-terminus was expressed in *E. coli* BL21(DE3) by induction with 1 mM IPTG and purified by Ni^{2+} affinity chromatography. The results of SDS-PAGE and Western blot showed that the purified CysE protein had an expected molecular weight of 24.6 kDa (Fig. 2B and C).

3.2. Serine acetyltransferase activity of CysE protein

As shown in Fig. 3A, serine acetyltransferase activity of CysE catalyzed the formation of OAS along with CoA from L-Ser and AcCoA. Serine acetyltransferase activity of CysE was detected using DTNB colorimetric assay. The reaction showed an obvious color change from clear to yellow after DTNB reagent was added, and the OD value at 405 nm was obtained. The specific activity of the CysE was 3.8098 ± 0.03 μmol/min/mg. The product CoA in the enzymatic reaction of CysE protein was detected by HPLC analysis (Fig. 3B). The results demonstrated that CysE protein had the serine acetyltransferase activity. Compared with HPLC assay, DTNB colorimetric assay was more efficient and was utilized for kinetic studies of CysE.

The Z-factor described the sensitivity and reproducibility of an assay. The Z-factor of a good assay should be greater than 0.5 and less than 1 [24,32]. The results showed that the mean and standard deviation values of OD_{405} were 0.2396 and 0.0049 from the 60 positive controls and 0.1263 and 0.0063 from the 60 negative controls, respectively. The Z-factor of 0.7034 was obtained for the assay, which indicated that the assay was suitable for screening of CysE inhibitors.

3.3. Kinetic properties of CysE

The kinetic properties of CysE were determined using DTNB colorimetric assay. From time course and enzyme concentration curves, the initial velocity of CysE was determined in 5 min and its optimal concentration was 4 μg/ml (Supplement figure 1A and Supplement figure 1B). The CysE activity was determined at varying pH with appropriate buffer systems (4–10) and different temperature from 16 to 80 °C. The results showed that CysE had maximal activity at pH 7.5 (Fig. 4A) and at the temperature of 37 °C (Fig. 4B). The enzymatic activity of CysE was not significantly changed by varying the Mg^{2+}, Ca^{2+}, Ba^{2+} and K^{+} concentration (Supplement Fig. 1C–F), indicating that the CysE activity did not rely on Mg^{2+}, Ca^{2+}, Ba^{2+} and K^{+}. The K_m and V_{max} values of CysE against substrates AcCoA and L-Ser were determined from the double reciprocal plots (Fig. 4C). The K_m and V_{max} against L-Ser were 0.4587 ± 0.0982 mM and 0.0137 ± 0.0012 mM/min, respectively, while the K_m and V_{max} against AcCoA were 0.2956 ± 0.01374 mM and 0.0170 ± 0.0008 mM/min, respectively (Fig. 4D).

3.4. Homology model building and molecular docking of CysE

The homology model of CysE was built by using SWISS-MODEL and the interaction between CysE and L-Ser (Fig. 5A) was investigated by Autodock (version 4.2). As shown in Fig. 5A, docking simulation results revealed the interactions between L-Ser and amino acid residues of CysE. The structure of CysE bound by L-Ser was expressed as CysE (L-Ser). Three amino acid residues (Asp29, Asp94 and His95) formed three H-bonds with L-Ser. Two-dimensional representation of these interactions, plotted by LIGPLOT [28], was shown in Fig. 5B. In addition, Lys128, Arg129 and Asn148 which were predicted interaction sites, formed H-bonds or ionic bonds with L-Ser. Therefore, Asp29, Asp94, His95, Lys128, Arg129 and Asn148 were likely to play a crucial role in the activity of CysE.

According to molecular docking data, six residues (Asp29, Asp94, His95, Lys128, Arg129 and Asn148) of CysE, which were showed to be bound with L-Ser, were substituted by alanine. CysE mutant proteins Asp94Ala, His95Ala, Lys128Ala, Arg129Ala and Asn148Ala were expressed and purified. Unfortunately, soluble Asp29Ala failed to be expressed. The results revealed that five CysE mutant proteins lost their acetyltransferase activity at different degrees (Fig. 5C). The specific activity of mutant proteins was showed Table 1. The results provided further evidence for the critical role of those five residues in binding of CysE and L-Ser.

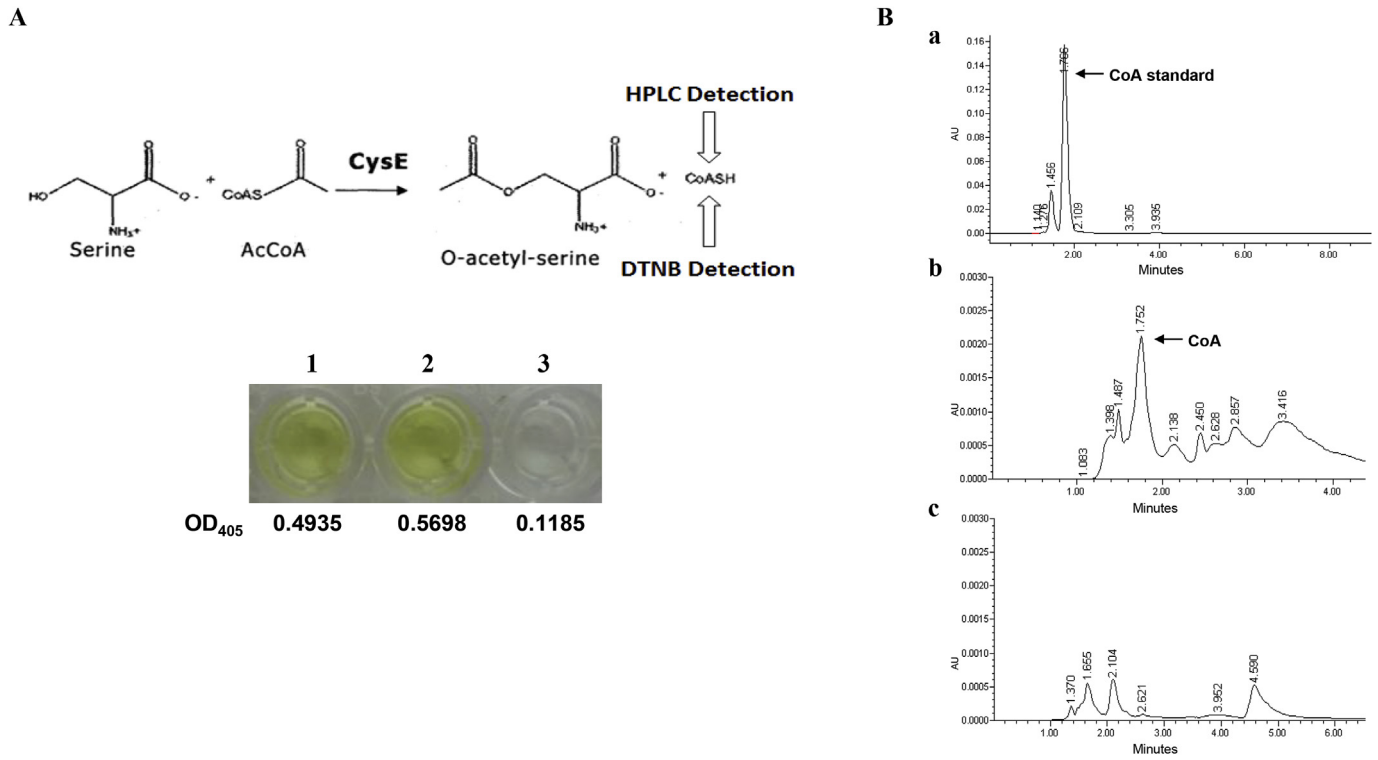

Fig. 3. Detection of serine acetyltransferase activity of CysE protein by DTNB colorimetric assay (A) and HPLC assay (B). A. 1. Enzymatic reaction of MRSA CysE (4 μg/ml); 2. The reaction lacking MRSA CysE protein and substrates but containing 200 μM CoA; 3. Negative control, the reaction lacking MRSA CysE protein. B. (a) CoA standard; (b) Enzymatic reaction of MRSA CysE protein (4 μg/ml); (c) The reaction containing all reactants except MRSA CysE protein as a control.

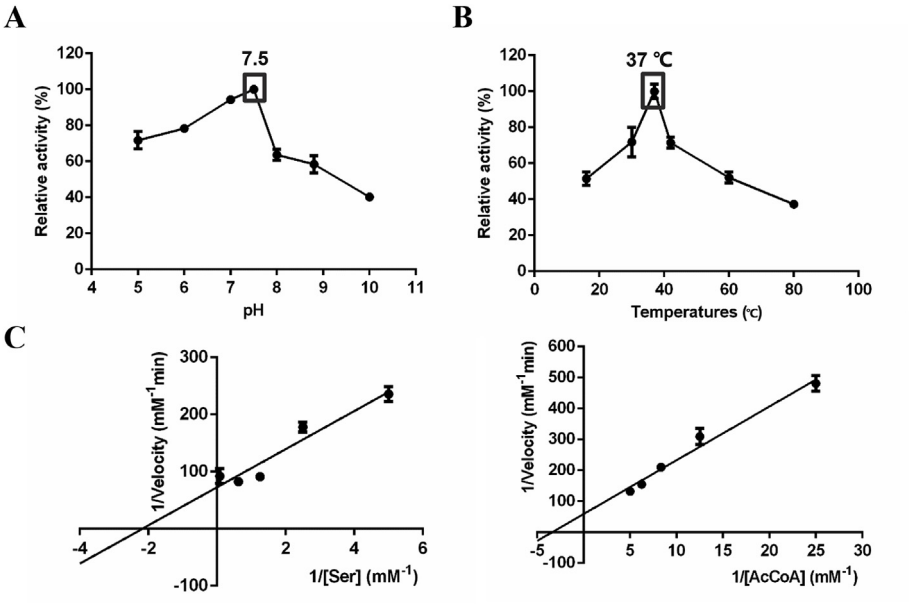

D

Substrate	*Km*(mM)	*Vmax*(mM min^{-1})	*Kcat*(s^{-1})	*Kcat/Km*($mM^{-1}s^{-1}$)
L-Ser	0.4587±0.0982	0.0137±0.0012	1.3601±0.1149	2.9651±0.3917
AcCoA	0.2956±0.01374	0.0170±0.0008	1.6830±0.7928	5.6936±0.3654

Fig. 4. Determination of the effect of pH (A) and temperature (B) on the activity of MRSA CysE and determination of Km and Vmax of MRSA CysE enzyme against L-Ser and AcCoA (C and D) from double reciprocal plot.

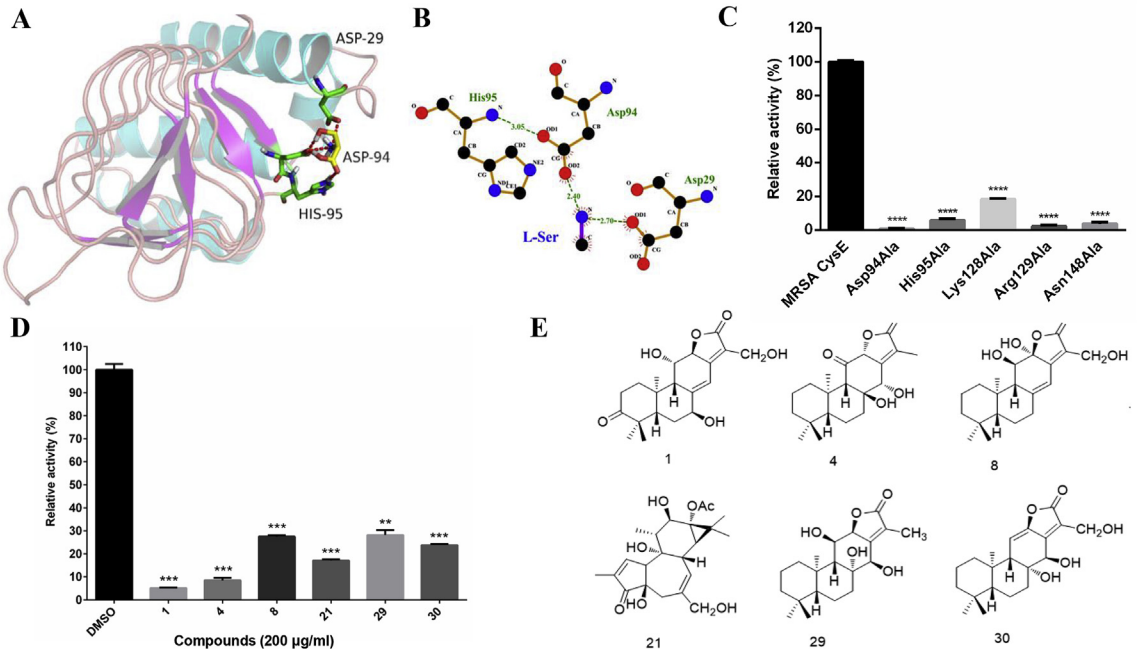

Fig. 5. Post-docking interactions between active site residues of protein (MRSA CysE) with ligand (L-Ser). The protein was depicted in cartoon view and ligand L-Ser as stick in the binding state (A); Interactions of CysE and the L-Ser by Ligplot (B); The specific activity of different MRSA CysE mutants (C); The inhibitory effect of six compounds on MRSA CysE activity (D) and the structural formula of six compounds (E). C. Differences among groups were calculated by unpaired two-tailed *t*-test. The asterisks represented the statistical differences between the relative activity of MRSA CysE and MRSA CysE mutants. ****, $P < 0.0001$. D. Differences among groups were calculated by unpaired two-tailed *t*-test. The asterisks represented the statistical differences between the relative activity of MRSA CysE in DMSO group and different compound treated groups. **, $P < 0.01$; ***, $P < 0.001$.

3.5. Identification of CysE inhibitors from natural product library

The DTNB colorimetric assay was used to screen CysE inhibitors. Six compounds exhibited inhibitory activity against CysE (Fig. 5D). The IC_{50} of compounds 1 (6β,11α,17-trihydroxyhelioscopinolide E), 4 (11-oxo-ebracteolatanolide B) and 30 ((4*R*,4a*R*)-dihydroxy-3-hydroxymethyl-7,7,10a-trimethyl-2,4,4a,5,6,6a,7,8,9,10,10a,l0b-dodecahydrophenanthro[3,2-*b*]furan-2-one) was 29.83 ± 0.2133, 71.84 ± 0.2678 and 71.84 ± 0.1495 μM, respectively. The structural formula of six compounds were shown in Fig. 5E.

3.6. Inhibitory effect of inhibitors on MRSA growth

The six inhibitors were subsequently tested for their efficacy against MRSA strain using resazurin assay. Compound 4 had the lowest MIC value (12.5 μg/ml) among these tested compounds, and the MIC value of compound 30 was 25 μg/ml (Fig. 6A and B). The MICs of compounds 1, 8 (7-deoxylangduin B), 21 (phorbol-13-acetate) and 29 (yuexiandajisu E) were 200, 50, 200 and 100 μg/ml respectively. The results indicated that compounds 4 and 30 were more effective in inhibiting the growth of MRSA. As positive controls, the MIC of vancomycin was 1 μg/ml and the MIC of clindamycin was 12.5 μg/ml. Compound 4 had the same MIC value with clindamycin.

MRSA was then treated with compounds 4 and 30 at 1 × MIC and 2 × MIC, respectively. Both growth curves (Fig. 7A and C) and CFU curves (Fig. 7B and D) of MRSA showed that the bacteria treated by 1 × MIC compounds 4 and 30 grew slowly rather than control group. When the concentration of compounds reached to 2 × MIC, they exhibited more obviously inhibitory effect on MRSA growth.

3.7. Inhibition types of CysE inhibitors

The inhibitory constant (Ki) and inhibition types of compounds 4 and 30 on CysE were determined by double reciprocal plots (Fig. 8A and Table 2). Kinetic parameters of compound 4 on CysE showed that the inhibition was mixed with L-Ser and competitive with AcCoA. However, compound 30 was competitive with L-Ser and mixed with AcCoA. The docking results of CysE and compounds revealed that those two compounds formed hydrogen bonds with Ala43, Gly44 and His95, whereas compound 30 formed hydrogen bonds with Asp94 (Fig. 8B). This indicated that these amino acid residues of CysE were action sites of two compounds.

3.8. Inhibitory effect of compounds 4 and 30 on MRSA biofilm

As shown in Fig. 6C and D, compounds 4 and 30 were also effective in destroying MRSA biofilm after treatment at the MIC value and 2 × MIC value for 48 h compared to controls. Compound 30 showed better inhibition for biofilm compared to compound 4.

3.9. Cytotoxicity of compounds 4 and 30

Since compounds 4 and 30 exhibited inhibitory effects on MRSA growth, we evaluated whether these compounds had toxicity to mammalian cells. Cytotoxicity of compounds 4 and 30 on human macrophage cell THP-1 and mouse macrophage cell RAW264.7 was tested

Table 1
The specific activity of five MRSA CysE mutants.

Mutants	WT CysE	Asp94	His95	Lys128	Arg129	Asn148
Specific activity (nmol/min/mg)	3.8098 ± 0.0243	0.0304 ± 0.0052	0.2184 ± 0.0289	0.6962 ± 0.0162	0.0812 ± 0.0244	0.1405 ± 0.0312

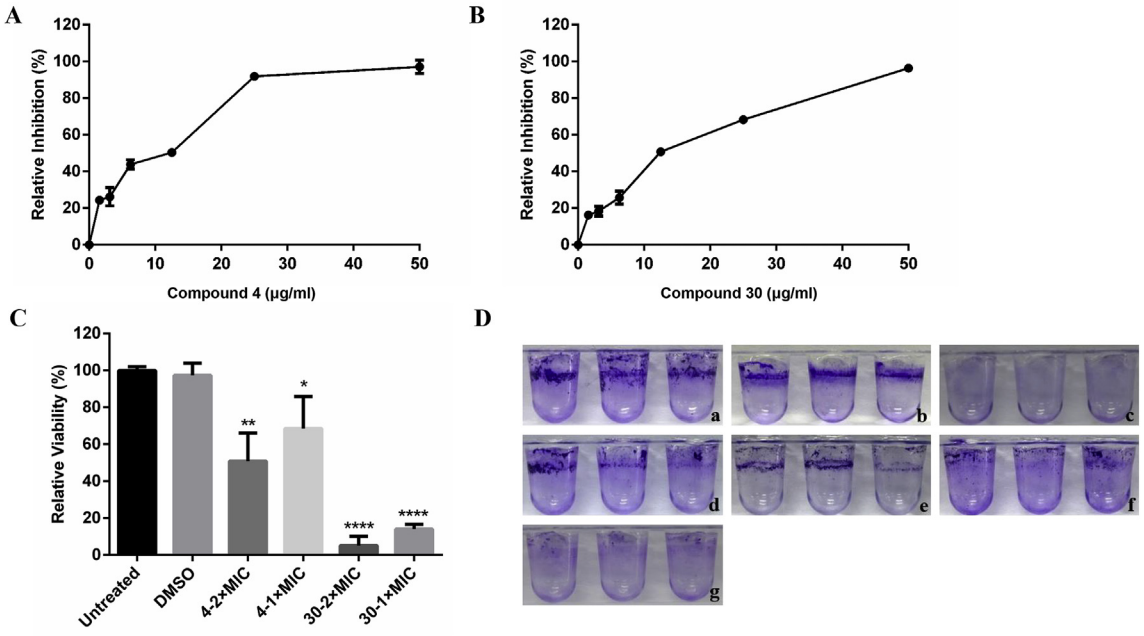

Fig. 6. The inhibitory effect of different compounds on the growth of MRSA (A and B) and MRSA biofilm (C and D). The value of crystal violet uptake (C) and polystyrene wells stained by crystal violet (D). a. MRSA; b. MRSA with DMSO; c. TSB medium without MRSA (control); d. MRSA treated with compound 4 at 2 × MIC; e. MRSA treated with compound 4 at 1 × MIC; f. MRSA treated with compound 30 at 2 × MIC; g. MRSA treated with compound 30 at 1 × MIC. C. Differences among groups were calculated by unpaired two-tailed *t*-test. The asterisks represented the statistical differences between the relative viability of MRSA in untreated group and different compound treated groups. *, $P < 0.05$; **, $P < 0.01$; ***, $P < 0.001$. (For interpretation of the references to color in this figure legend, the reader is referred to the Web version of this article.)

respectively. The results showed that compounds 4 and 30 had weak cytotoxicity (with more than 80% cell viability) on both THP-1 and RAW264.7 macrophage cells (Supplement Figure 2).

4. Discussion

The emergence of antibiotic resistance on *Staphylococcus aureus* has greatly aroused people's attention. The identification of more novel compounds targeting specific enzymes will provide more drug candidates for developing effective anti-*S. aureus* and MRSA drugs. In recent years, sulfur metabolic pathways like cysteine biosynthetic provide a new probability for therapeutic intervention in treating bacterial infections [8].

Sulfur is a significant element for life and plays an important role in microbial metabolic processes. Many enzymes encoded by genes *cysNC*, *cysD*, *cysQ*, *sirA* and *subI*, etc. Were involved in the metabolism of sulfur and up-regulated when bacteria faced with oxidative stress, nutrient starvation, dormancy adaptation, and survival [8,33,34]. Sulfur

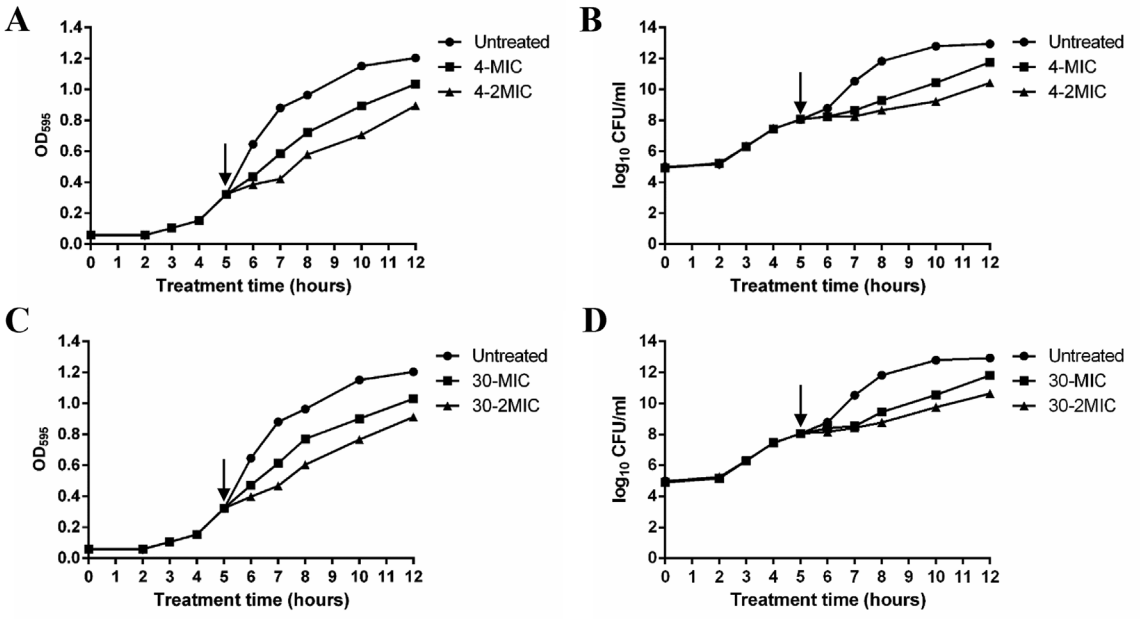

Fig. 7. The growth curve (A and C) and CFU (B and D) of MRSA. The MRSA cultures were grown in TSB medium with different concentration of compound 4 (A and B) and compound 30 (C and D). The OD_{595} value and CFU were monitored at the interval of 1h. The arrow indicated the time point when compound was treated.

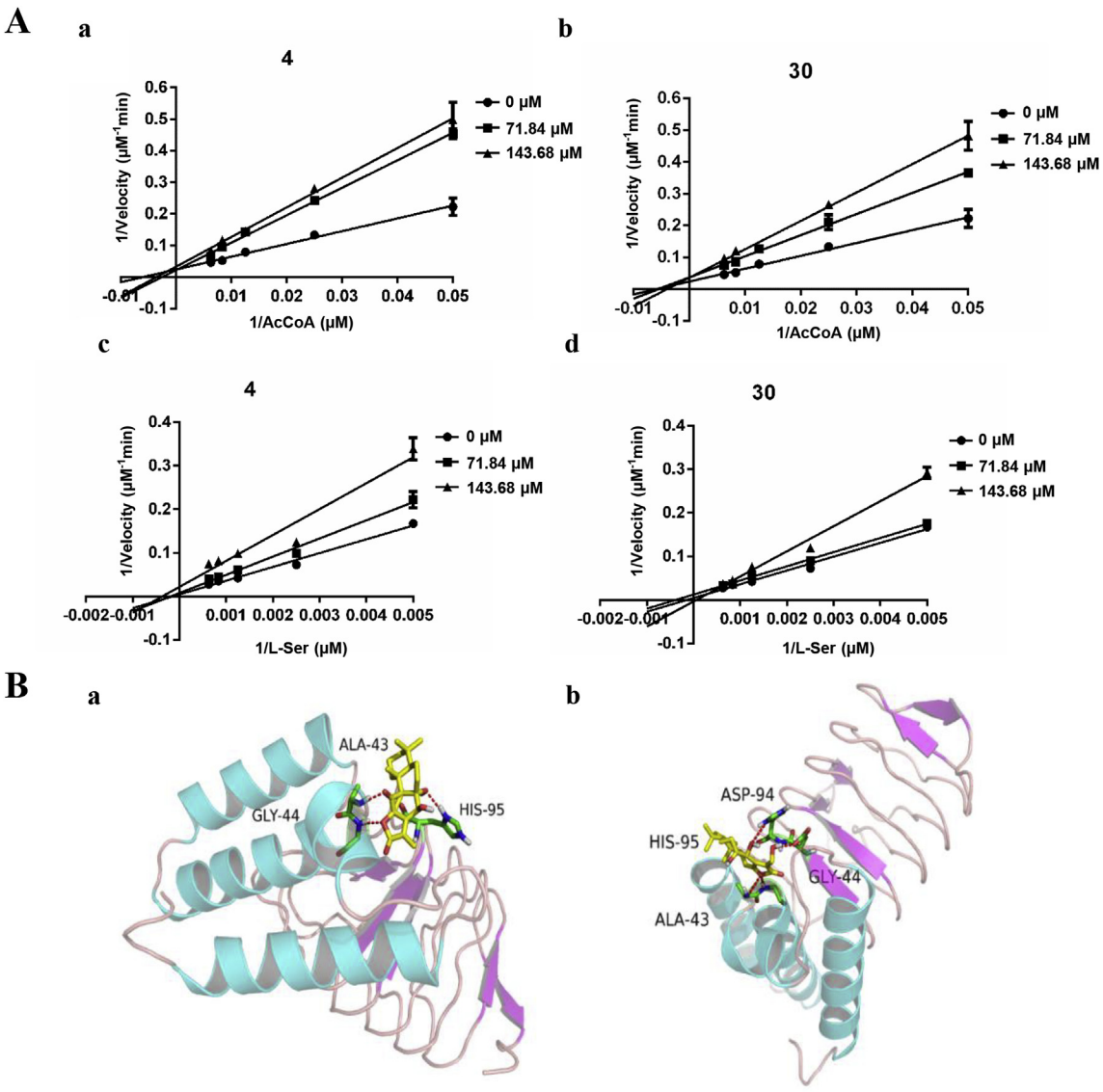

Fig. 8. The inhibition types of different compounds on MRSA CysE (A) and Post-docking interactions between active residues of MRSA CysE with compounds 4 and 30 respectively (B).

Table 2
The inhibition types of different inhibitors on MRSA CysE.

Compounds	K_i (μM)			
	$K_{i\text{-}com}$/L-Ser	$K_{i\text{-}non}$/L-Ser	$K_{i\text{-}com}$/AcCoA	$K_{i\text{-}non}$/AcCoA
4	225.3896	107.1599	53.8975	—
30	47.6583	—	111.5701	130.6895

metabolic can be divided into sulfation branch and reductive branch. In its reduced branch, sulfur is involved in the biosynthesis of the amino acids cysteine and methionine [34]. The biosynthesis of cysteine occurs via serine acetyltransferase CysE and O-acetylserine sulfhydrylase CysK. Turnbull et al. reported that elevated *cysE* expression brought about more resistance to oxidative stress and antibiotics [18]. Microbial pathogens such as *M. tuberculosis* can survive in complicated and hostile environmental conditions, including nutrient deprivation, high levels of oxidative stress and low pH of the host macrophage. The infected bacteria under these conditions require the coordinated regulation of gene expression to survive [35]. Rengarajan et al. used a microarray-based technique to identify 126 genes which were necessary to survival of *M. tuberculosis* in macrophages. One of those genes was *cysE,* which was essential for survival in a mouse model of *M. tuberculosis* infection [20]. In addition, inactivation of the *cysB* gene (CysB was the major positive regulator of cysteine biosynthesis) and a resulting disruption of cysteine biosynthesis were found to be the major mechanism of amdinocillin resistance in clinical isolates of *E. coli* [36]. Therefore, it is necessary for us to deeply understand the synthesis of cysteine and CysE properties, which is helpful in finding CysE inhibitors.

A colorimetric assay for detection of CysE activity was developed allowing us to measure kinetic properties of CysE and screen CysE inhibitor from natural products in this study. Six compounds exhibited inhibition on CysE activity and MRSA growth. Compounds 4 and 30 of them exhibited better inhibitory effect on CysE activity and MRSA growth. To confirm the specificity those two compounds on acetyltransferase of CysE, we tested whether they were capable to act on the acetyltransferase activity of *S. aureus* GlmU which is a bifunctional enzyme with glucosamine-1-phosphate acetyltransferase activity and N-acetylglucosamine-1-phosphate uridyltransferase activity in UDP-GlcNAc biosynthetic pathway. GlmU acetyltransferase activity catalyzes the conversion of substrates glucosamine-1-phosphate and acetyl coenzyme A to products N-actylglcosamine-1-phosphate and coenzyme

A. However, the results showed that compounds 4 and 30 were unable to inhibit *S. aureus* GlmU acetyltransferase activity (unpublished data in our laboratory). This suggested that compounds 4 and 30 were specifically targeting CysE.

The consistent results in the kinetic and docking analyses were also found. Kinetic studies of compound 4 on CysE showed that the inhibition was mixed with L-Ser and competitive with AcCoA. Compound 30 exhibited competitive with L-Ser and mixed with AcCoA. In addition, the docking results revealed that the key residue His95 was predicted to form hydrogen bonds with the two inhibitors. That means the inhibitors competed with the binding sites of substrates L-Ser. It is helpful for us to understand the action sites of the inhibitors through docking.

Previous studies had shown that many bacteria like *S. aureus* produced a multilayered biofilm consisting of glycocalyx and slime layers with heterogeneous protein expression throughout [37,38]. The bacterial biofilm is regarded as a microbially-derived sessile community and are embedded in a matrix of extracellular polymeric substance. Once establishing the biofilm, the bacteria were recalcitrant to the host response and antimicrobial treatment, and turned into etiological agent of many recurrent infections like osteomyelitis, indwelling medical device infection, periodontitis, chronic wound infection, chronic rhinosinusitis, endocarditis and ocular infection [20]. Therefore, attempts to develop an effective anti-*Staphylococcus aureus* biofilm drug are also required. In this study, we also found that compound 4 and 30 could destroy the MRSA biofilm, which would provide some insights to develop novel drugs against bacterial biofilm.

Taken together, CysE was encoded by the *cysE* gene in the methicillin-resistant *Staphylococcus aureus*. CysE was characterized in terms of optimal catalytic conditions, kinetic parameters and active sites. Six compounds inhibiting CysE activity were found. They also had inhibitory effect on MRSA growth and two of them were capable to destroy mature MRSA biofilm. The binding sites of compound 4 and 30 to CysE protein were revealed by molecular docking. The compounds 4 and 30 as inhibitors on CysE, MRSA and MRSA biofilm may offer structural basis for new anti-*S. aureus* and anti-MRSA drugs.

Declaration

We declare that we have no conflict of interest and the work described has not been published previously.

Acknowledgements

The present study was supported by the National Natural Science Foundation of China (81573469 and 81872970).

Appendix A. Supplementary data

Supplementary data to this article can be found online at https://doi.org/10.1016/j.micpath.2019.04.002.

References

[1] S.K. Fridkin, J.C. Hageman, M. Morrison, L.T. Sanza, K. Como-Sabetti, J.A. Jernigan, et al., Methicillin-resistant Staphylococcus aureus disease in three communities, N. Engl. J. Med. 352 (2005) 1436–1444.
[2] B.A. Diep, Q. Phung, S. Date, D. Arnott, C. Bakalarski, M. Xu, et al., Identifying potential therapeutic targets of methicillin-resistant Staphylococcus aureus through in vivo proteomic analysis, J. Infect. Dis. 209 (2014) 1533–1541.
[3] M.C. Enright, D.A. Robinson, G. Randle, E.J. Feil, H. Grundmann, B.G. Spratt, The evolutionary history of methicillin-resistant Staphylococcus aureus (MRSA), Proc. Natl. Acad. Sci. U. S. A. 99 (2002) 7687–7692.
[4] S.R. Gill, D.E. Fouts, G.L. Archer, E.F. Mongodin, R.T. Deboy, J. Ravel, et al., Insights on evolution of virulence and resistance from the complete genome analysis of an early methicillin-resistant Staphylococcus aureus strain and a biofilm-producing methicillin-resistant Staphylococcus epidermidis strain, J. Bacteriol. 187 (2005) 2426–2438.
[5] G.J. Moran, A. Krishnadasan, R.J. Gorwitz, G.E. Fosheim, L.K. McDougal, R.B. Carey, et al., Methicillin-resistant S. aureus infections among patients in the emergency department, N. Engl. J. Med. 355 (2006) 666–674.
[6] E. Nannini, B.E. Murray, C.A. Arias, Resistance or decreased susceptibility to glycopeptides, daptomycin, and linezolid in methicillin-resistant Staphylococcus aureus, Curr. Opin. Pharmacol. 10 (2010) 516–521.
[7] S.J. Peacock, G.K. Paterson, Mechanisms of methicillin resistance in Staphylococcus aureus, Annu. Rev. Biochem. 84 (2015) 577–601.
[8] H. Paritala, K.S. Carroll, New targets and inhibitors of mycobacterial sulfur metabolism, Infect. Disord. - Drug Targets 13 (2013) 85–115.
[9] M.I. Voskuil, I.L. Bartek, K. Visconti, G.K. Schoolnik, The response of mycobacterium tuberculosis to reactive oxygen and nitrogen species, Front. Microbiol. 2 (2011) 105.
[10] M.A. Forrellad, L.I. Klepp, A. Gioffre, Y. Sabio, J. Garcia, H.R. Morbidoni, M. de la Paz Santangelo, et al., Virulence factors of the Mycobacterium tuberculosis complex, Virulence 4 (2013) 3–66.
[11] T. Hampshire, S. Soneji, J. Bacon, B.W. James, J. Hinds, K. Laing, et al., Stationary phase gene expression of Mycobacterium tuberculosis following a progressive nutrient depletion: a model for persistent organisms? Tuberculosis 84 (2004) 228–238.
[12] N.M. Kredich, G.M. Tomkins, The enzymic synthesis of L-cysteine in Escherichia coli and Salmonella typhimurium, J. Biol. Chem. 241 (1966) 4955–4965.
[13] J. Qiu, D. Wang, Y. Ma, T. Jiang, Y. Xin, Identification and characterization of serine acetyltransferase encoded by the Mycobacterium tuberculosis Rv2335 gene, Int. J. Mol. Med. 31 (2013) 1229–1233.
[14] Y. Haitani, N. Awano, M. Yamazaki, M. Wada, S. Nakamori, H. Takagi, Functional analysis of L-serine O-acetyltransferase from Corynebacterium glutamicum, FEMS Microbiol. Lett. 255 (2006) 156–163.
[15] S. Kumar, I. Raj, I. Nagpal, N. Subbarao, S. Gourinath, Structural and biochemical studies of serine acetyltransferase reveal why the parasite Entamoeba histolytica cannot form a cysteine synthase complex, J. Biol. Chem. 286 (2011) 12533–12541.
[16] E. Salsi, B. Campanini, S. Bettati, S. Raboni, S.L. Roderick, P.F. Cook, et al., A two-step process controls the formation of the bienzyme cysteine synthase complex, J. Biol. Chem. 285 (2010) 12813–12822.
[17] T. Wang, T.S. Leyh, Three-stage assembly of the cysteine synthase complex from Escherichia coli, J. Biol. Chem. 287 (2012) 4360–4367.
[18] A.L. Turnbull, M.G. Surette, Cysteine biosynthesis, oxidative stress and antibiotic resistance in Salmonella typhimurium, Res. Microbiol. 161 (2010) 643–650.
[19] R. Schnell, D. Sriram, G. Schneider, Pyridoxal-phosphate dependent mycobacterial cysteine synthases: structure, mechanism and potential as drug targets, Biochim. Biophys. Acta 1854 (2015) 1175–1183.
[20] N.K. Archer, M.J. Mazaitis, J.W. Costerton, J.G. Leid, M.E. Powers, M.E. Shirtliff, Staphylococcus aureus biofilms: properties, regulation, and roles in human disease, Virulence 2 (2011) 445–459.
[21] S. Dastgheyb, J. Parvizi, I.M. Shapiro, N.J. Hickok, M. Otto, Effect of biofilms on recalcitrance of staphylococcal joint infection to antibiotic treatment, J. Infect. Dis. 211 (2015) 641–650.
[22] P. Francois, D. Pittet, M. Bento, B. Pepey, P. Vaudaux, D. Lew, et al., Rapid detection of methicillin-resistant Staphylococcus aureus directly from sterile or nonsterile clinical samples by a new molecular assay, J. Clin. Microbiol. 41 (2003) 254–260.
[23] Y. Zhou, Y. Xin, S. Sha, Y. Ma, Kinetic properties of Mycobacterium tuberculosis bifunctional GlmU, Arch. Microbiol. 193 (2011) 751–757.
[24] C.M. Sassetti, D.H. Boyd, E.J. Rubin, Genes required for mycobacterial growth defined by high density mutagenesis, Mol. Microbiol. 48 (2003) 77–84.
[25] P.J. Brennan, Structure, function, and biogenesis of the cell wall of Mycobacterium tuberculosis, Tuberculosis 83 (2003) 91–97.
[26] X. Shi, S. Sha, L. Liu, X. Li, Y. Ma, A 96-well microtiter plate assay for high-throughput screening of Mycobacterium tuberculosis dTDP-d-glucose 4,6-dehydratase inhibitors, Anal. Biochem. 498 (2016) 53–58.
[27] G.M. Morris, R. Huey, W. Lindstrom, M.F. Sanner, R.K. Belew, D.S. Goodsell, et al., AutoDock4 and AutoDockTools4: automated docking with selective receptor flexibility, J. Comput. Chem. 30 (2009) 2785–2791.
[28] A.C. Wallace, R.A. Laskowski, J.M. Thornton, LIGPLOT: a program to generate schematic diagrams of protein-ligand interactions, Protein Eng. 8 (1995) 127–134.
[29] C.J. Wang, Q.L. Yan, Y.F. Ma, C.P. Sun, C.M. Chen, X.G. Tian, et al., Ent-Abietane and Tigliane Diterpenoids from the Roots of Euphorbia Fischeriana and Their Inhibitory Effects against Mycobacterium Smegmatis, (2017).
[30] M.A. Jyoti, K.W. Nam, W.S. Jang, Y.H. Kim, S.K. Kim, B.E. Lee, et al., Antimycobacterial activity of methanolic plant extract of Artemisia capillaris containing ursolic acid and hydroquinone against Mycobacterium tuberculosis, J. Infect. Chemother. 22 (2016) 200–208.
[31] M.A. Jyoti, T. Zerin, T.H. Kim, T.S. Hwang, W.S. Jang, K.W. Nam, et al., In vitro effect of ursolic acid on the inhibition of Mycobacterium tuberculosis and its cell wall mycolic acid, Pulm. Pharmacol. Therapeut. 33 (2015) 17–24.
[32] Ji-Hu Zhang TDYC, Kevin R. Oldenburg, A simple statistical parameter for use in evaluation and validation of high throughput screening assays, J. Biomol. Screen 4 (1999) 67–73.
[33] H.W. Boucher, G.H. Talbot, J.S. Bradley, J.E. Edwards, D. Gilbert, L.B. Rice, et al., Bad bugs, no drugs: no ESKAPE! an update from the Infectious Diseases Society of America, Clin. Infect. Dis. 48 (2009) 1–12.
[34] D.P. Bhave, W.B. Muse 3rd, K.S. Carroll, Drug targets in mycobacterial sulfur metabolism, Infect. Disord. - Drug Targets 7 (2007) 140–158.
[35] C. Nathan, M.U. Shiloh, Reactive oxygen and nitrogen intermediates in the relationship between mammalian hosts and microbial pathogens, Proc. Natl. Acad. Sci. U. S. A. 97 (2000) 8841–8848.
[36] E. Thulin, M. Sundqvist, D.I. Andersson, Amdinocillin (Mecillinam) resistance mutations in clinical isolates and laboratory-selected mutants of Escherichia coli, Antimicrob. Agents Chemother. 59 (2015) 1718–1727.
[37] L. Hall-Stoodley, J.W. Costerton, P. Stoodley, Bacterial biofilms: from the natural environment to infectious diseases, Nat. Rev. Microbiol. 2 (2004) 95–108.
[38] K.K. Jefferson, What drives bacteria to produce a biofilm? FEMS Microbiol. Lett. 236 (2004) 163–173.